Geophysical Research Letters

RESEARCH LETTER
10.1029/2020GL091764

Data-Driven Clustering Reveals More Than 900 Small Magnitude Slow Earthquakes and Their Characteristics

C. Aiken[1] and K. Obara[2]

[1]Ifremer Centre de Bretagne - REM – GM – LAD, Plouzané, France, [2]Earthquake Research Institute, University of Tokyo, Tokyo, Japan

Key Points:

- More than 900 small magnitude slow earthquakes detected via data-driven clustering of tremor and low-frequency earthquake catalogs
- Small magnitude slow earthquakes share similar scaling properties to their larger counterparts and may be sub-episodes of larger events
- Slow earthquakes of all sizes exhibit similar inter-event rupture speed, meaning it does not control spatial extent or eventual magnitude

Supporting Information:

Supporting Information may be found in the online version of this article.

Correspondence to:

C. Aiken,
chastity.aiken@ifremer.fr

Citation:

Aiken, C., & Obara, K. (2021). Data-driven clustering reveals more than 900 small magnitude slow earthquakes and their characteristics. *Geophysical Research Letters*, *48*, e2020GL091764. https://doi.org/10.1029/2020GL091764

Received 20 NOV 2020
Accepted 18 MAY 2021

Author Contributions:

Conceptualization: C. Aiken
Data curation: C. Aiken
Formal analysis: C. Aiken
Investigation: C. Aiken
Methodology: C. Aiken
Project Administration: C. Aiken, K. Obara
Software: C. Aiken
Validation: C. Aiken, K. Obara
Writing – original draft: C. Aiken, K. Obara
Writing – review & editing: C. Aiken, K. Obara

Abstract Small magnitude slow earthquakes remain largely undetected in geodetic data due to noise levels. However, tremor and low-frequency earthquakes (LFE) may manifest slowly slipping fault motion as a cluster of events, i.e., a slow earthquake. Here, we identify >900 slow earthquakes in southwest Japan via data-driven clustering of tremor and LFE catalogs. We establish a more complete database for slow earthquakes in southwest Japan and demonstrate their characteristics and long-term behavior. While sometimes sub-episodes of well-known episodic tremor and slip, the small slow earthquake clusters share similar scaling properties–energy, duration, and rupture area–with larger magnitude fast and slow earthquakes. The small slow earthquake clusters tend to rupture faster when migrating in their preferred rupture direction, but inter-event rupture speeds are on average similar to those of larger slow earthquakes. This suggests that rupture speed does not necessarily control slow earthquake spatial extent or eventual magnitude.

Plain Language Summary Slow earthquakes release a similar amount of energy as fast earthquakes but over a much longer time scale. While this difference makes them less dangerous to the public, their frequent occurrence signals that faults move almost continuously. In this study, we apply a technique to group seismic events in southwest Japan into clusters that represent slow earthquake phenomena. We use these slow earthquake clusters to investigate fault behavior in the long-term and their characteristics as compared to other slow earthquake phenomena. We found that the slow earthquakes are small in size, but their properties scale similarly to larger slow earthquakes and fast earthquakes in energy, duration, and ruptured area, suggesting that the slow earthquakes are fractal in nature. However, how fast the slow earthquakes rupture does not indicate how big they can become, in either their energy released or spatial spread.

1. Introduction

The discovery of slow earthquakes (Dragert et al., 2001; Obara, 2002) has redefined our understanding of seismic behavior from a slow versus fast slip to a spectra of seismic slip (Peng & Gomberg, 2010). Slow earthquakes can release a similar amount of energy as regular fast earthquakes, albeit over a much longer time scale (Ide et al., 2007; Peng & Gomberg, 2010). While this slow energy release does not make slow earthquakes dangerous to the public, their existence signifies the accumulation and release of stress on faults at an occurrence rate far more often than earthquakes of equal magnitude. Four phenomena are considered as a part of the slow earthquake family: tectonic tremor, low-frequency earthquakes (LFEs), very low-frequency earthquakes, and slow slip events, where a tectonic tremor episode can be expressed as a swarm of LFEs (Shelly et al., 2007). When tremor, LFEs, and slow slip are simultaneously observed in seismic and geodetic data, the event is termed episodic tremor and slip (ETS) (Obara et al., 2004; Rogers & Dragert, 2003). However, sometimes tremor and LFEs are observed without geodetic signature. This is because tremor and LFEs are easier to detect by seismic networks than slow slip that is on geodetic instrumentation due to noise. Even without geodetically observed slip, tremor and LFEs are treated as a manifestation of a slow slip event (Shelly et al., 2011), as tremor and LFEs can closely track slow slip events in space and time (Bartlow et al., 2011; Frank et al., 2015; Hirose & Obara, 2010).

In southwest Japan, slow earthquakes have been observed at 25–50 km depths along the Nankai subduction zone (Obara, 2002; Ozawa et al., 2002; Obara et al., 2004). In particular, slow earthquake episodes in Western Shikoku are usually composed of short-term slow slip events, tremor, and LFEs and occur about

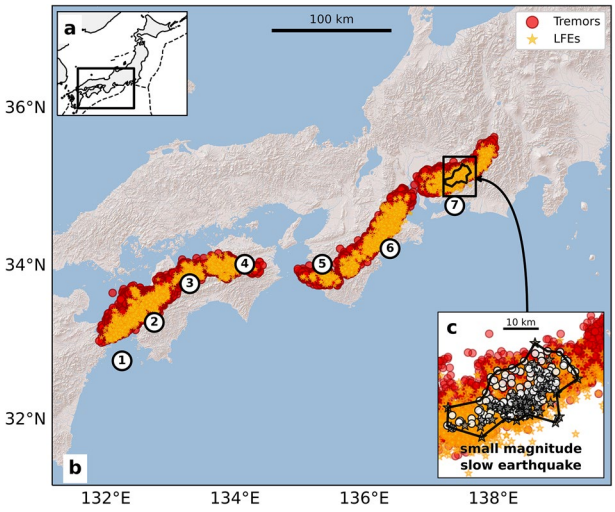

Figure 1. Map view of data used in this study and example of a detected slow earthquake cluster (SEC). (a) Study area (black box) is located in southwest Japan, with plate boundaries marked at Earth's surface (dashed black lines). (b) Study area showing selected tremor and low-frequency earthquake events (circles and stars, respectively); circled numbers mark different regions along the Nankai subduction zone: **1** - Bungo Channel, **2** - Western Shikoku Island, **3** - Central Shikoku Island, **4** - Eastern Shikoku Island, **5** - Southern Kii Peninsula, **6** - Northern Kii Peninsula, **7** – Tokai. (c) Map view of a small magnitude SEC detected in the Tokai region that began 19 June 2004. Its tremor (white circles) and low-frequency earthquakes (gray stars) are shown. Black outline depicts the concave hull of the tremor and LFEs events comprising the SEC and therefore represents the SEC's apparent rupture area on the plate interface.

every 6 months (Obara, 2010; Obara et al., 2004). Most slow earthquake episodes that we know of today along the Nankai subduction zone have long durations, lasting several days and having magnitudes larger than *M*5.5 (Sekine et al., 2010). The linear relationship between the moment release of a slow slip event and the duration time or total number of tremor during each deeply seated episodic tremor and slip (ETS) event in Cascadia and Nankai suggests that small magnitude slow earthquakes are likely not detected geodetically but detected only seismically (Aguiar et al., 2009; Frank and Brodsky, 2019; Michel et al., 2019; Obara, 2010), and likewise, tend to be overlooked when pursuing in-depth knowledge of how faults behave.

Although efforts have been made to create slow earthquake databases (Kano et al., 2018), we still lack a complete record of slow earthquakes along the Nankai subduction zone, one that includes small magnitude slow earthquakes. We ask–what can small magnitude slow earthquakes tell us about Nankai subduction zone behavior? To answer this question, we use data-driven clustering methods to detect slow earthquakes in a 9-year tremor catalog (Idehara et al., 2014) and LFE catalog. We investigate the characteristics of the detected slow earthquakes, many of which have small magnitude, and compare our results to observations of regular (fast) earthquakes and known larger-sized slow earthquake phenomena around the world. Our aims are to form a more complete database of slow earthquakes in southwest Japan and bridge the gap of knowledge between small-scale and large-scale slow earthquakes.

2. Materials and Methods

Our data are two 9-year catalogs—tremor and LFEs—for the Nankai subduction zone (Figure 1). The tremor catalog contains 82,275 events between April 2004 and March 2013 (Idehara et al., 2014). The tremor has moment magnitudes and durations ranging from 10 to 300 s, and residual error is on average of 0.8 s. The LFE catalog is a subset of the Japan Meteorological Agency (JMA) unified hypocenter catalog. The LFEs have JMA magnitude and horizontal and depth errors of 1 and 2 km on average, respectively.

LFEs and tremor are considered to be equivalent representations of slow earthquake phenomena (e.g., Aiken & Peng, 2014). They are, however, detected by different methods. LFE is usually included in a tremor signal; however, sometimes LFEs are recorded as occurring independently of tremor or vice versa (e.g., Chestler & Creager, 2017). Therefore, in this study, we use the LFE catalog as a supplement for tremor. For consistency, we selected LFEs that lie within the same spatial and temporal boundaries as the tremor catalog, which resulted in ~20,000 LFEs (Figure 1).

We use spatio-temporally clustered tremor and LFE events as a proxy for slow earthquake phenomena via a two-step process, similar to Zaliapin and Ben-Zion (2013). In the first step, we identify nearest neighbors by treating each event in the catalog as the child of some parent event that occurs before, i.e., its nearest neighbor. Essentially, the nearest neighbor is the event that occurs before the child that also has the lowest $\eta = dt\ x\ dr$ value, where dt is time difference and dr is the Cartesian distance. We examine the space-time distributions of the nearest neighbors inherent to our tremor and LFE catalogs, separately (Figure S2). From the 2D-distributions of nearest neighbors, we determine the criteria that separates unrelated events and related events (i.e., close in time and space = related). We note that the clustering criteria for both catalogs are the same: $\eta_{max} = 1$, $dt_{max} = 4.8$ h (0.2 days), $dr_{max} = 15$ km. Therefore, we combined the tremor and LFE catalogs into one. In the second step, we treat each event in the combined catalog as a parent and find its children, forming clusters. For children that were also parents, these clusters were grouped together so that parents, children, and grandchildren formed a single unique cluster, i.e., a slow earthquake cluster

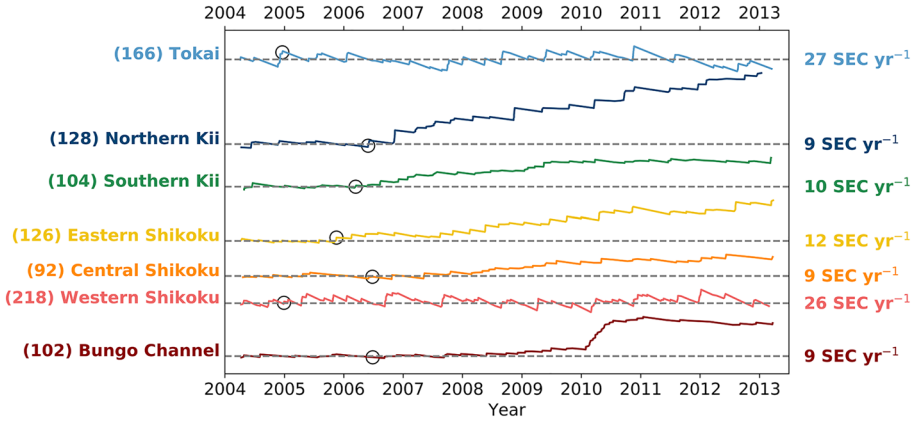

Figure 2. Detections and detrended rates of slow earthquake clusters (SECs) by region. West to east is shown from bottom to top; red to blue. Total number of SEC detections by region is in parentheses. The rate in each region used to detrend the cumulative detections was determined from the first 20 SECs in the time series (upper time limit shown as open circle). The trend rates for these times are the values listed on the right side and the dashed gray line represents those trends.

(Figure 1). With this data-driven clustering method, we identified 936 slow earthquake clusters (SECs) over the 9-year observation period (Aiken & Obara, 2021).

We investigate the slow earthquake clusters' magnitudes, durations, and rupture dimensions, directions, and speeds. We estimate their moment magnitudes from seismic moment (M_0), when reported. Otherwise, we assume M_{JMA} (JMA magnitude) is equivalent to M_L (local magnitude) and estimate M_0 from M_L using empirical relationship. Slow earthquake cluster duration is calculated simply as t_{last} - t_{first}, considering the duration of the final event in the slow earthquake cluster, when known. Slow earthquake cluster rupture dimensions are estimated from the concave hull of the clustered events in each slow earthquake cluster, providing an apparent ruptured area at Earth's surface (Figure 1c). We project the apparent ruptured area to the plate interface, assuming a dip of 30° (Ide, 2012), to estimate the "true" ruptured area. From the concave hull, we also estimated the length (L) and width (W) dimensions of the ruptured area—along the strike and perpendicular to the strike of the Nankai subduction zone, respectively—where width is also projected to the plate interface. While not exact, these adjustments provide more realistic values of the slow earthquake cluster rupture areas on the plate interface. Finally, we calculate their rupture directivity and speeds on both a micro-scale (between successive events) as well as macro-scale (all events). See Supporting Information for more details of the catalog, the clustering algorithm, and our calculations.

3. Characteristics of Detected Slow Earthquakes

3.1. Temporal Behavior

Our slow earthquake clusters (SECs) sometimes consisted of tremor and LFEs overlapping in space and time forming a single cluster of multiple event types (Figure 1c), representing the same physical process (Shelly et al., 2007). Other times, tremor and LFEs did not overlap in space and time and formed single-event type clusters of either tremors or LFEs (Figure S7), highlighting that sometimes slow earthquakes may be missed during automated detection processes. In isolating clusters with ≥20 events occurring along the Nankai subduction zone plate interface (Figure S4), we discovered 936 SECs occurring between 2004 and 2013 (Aiken & Obara, 2021). Each Nankai subduction zone region produced >90 SECs during the study period, but SEC occurrence rates differ throughout the observation period (Figure 2). Overall, the Western Shikoku and Tokai regions were the most active with relatively constant rates of 26 and 27 SEC year^{-1}, respectively. This aligns with Western Shikoku being an active "sweet spot" for repeating tremor episodes (Aiken et al., 2014). Other Nankai subduction zone regions exhibit nearly constant event rates between 2004 and 2006, ranging from 9 to12 SEC year^{-1}. However, after 2006, the SEC rates either increased to a new rate or increased and then returned to their "normal" 2004–2006 rate. Several regions demonstrated simultaneous rate increases after 2006. However, these rates are still much lower than the constantly high rates of Western Shikoku and

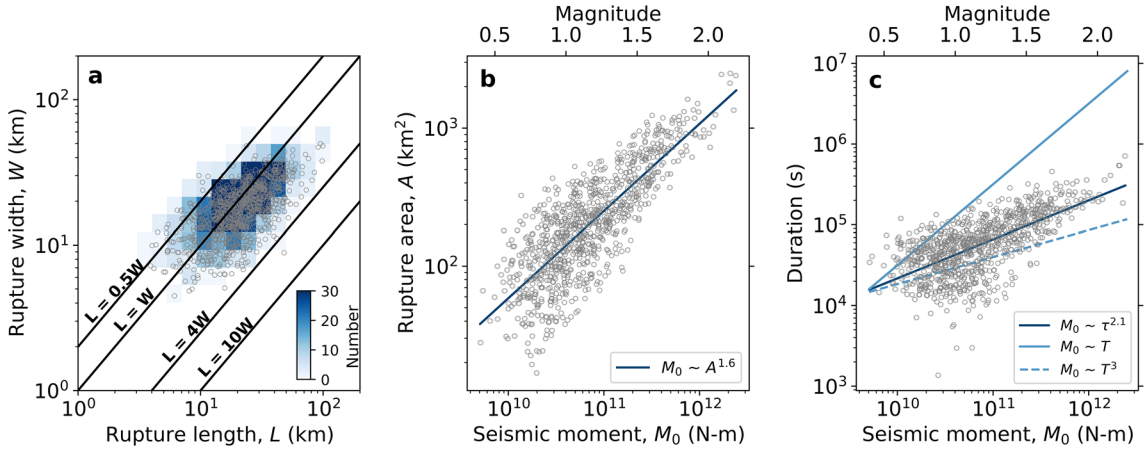

Figure 3. Slow earthquake cluster (SEC) scaling properties. (a) Rupture width versus length, (b) rupture area versus seismic moment and moment magnitude, and (c) seismic moment–duration scaling for the 936 slow earthquake clusters. In (a), the histogram count (number) is saturated at 30 to enhance visualization. Solid lines denote contours of constant aspect ratios. In (b), the data follow a trend (solid line) similar to what has been observed for regular earthquakes worldwide, i.e., $M_0 \sim A^{3/2}$ (Kanamori & Brodsky, 2004). Our fit is only slightly larger (1.6) with $r^2 = 0.65$. Rupture area shown in (b) is estimated from the concave hull approach with adjustment for fault dip (see Supporting Information). Rupture width shown in (a) is also adjusted for fault dip. In (c), the slow earthquakes weakly align with a $M_0 \sim \tau^2$ scaling; the fit has an $r^2 = 0.43$.

Tokai. We note that the rapid increase in SECs in the Bungo Channel around 2010 pertains to a known slow slip event (Hirose et al., 2010; Obara, 2010).

The Nankai subduction zone exhibited both stable sliding (smooth transition) and stick slip behaviors (sawtooth pattern) during the 2004–2013 period (Figure 2). Such patterns are typically indicative of continual aseismic slip (stable sliding) or the accumulation and release of stress when friction is overcome (stick-slip). Where smooth, the region is likely under high effective normal stress and slipping stably over time, as in the case of the 2010 Bungo Channel slow slip event (Hirose et al., 2010; Obara, 2010). In "sawtooth" times, multiple SECs occur nearly simultaneously in a single region, resulting in an uptick of SECs. During those periods, we have detected several SECs that are likely sub-episodes of known slow earthquake phenomena detected geodetically and/or seismologically, sometimes recognized as ETS. Tremor rate increase and 'sawtooth' patterns have been associated with recurring slow slip events, such as a M6 slow slip event in Mexico that was geodetically detected (Husker et al., 2019). Thus, our detected SECs are likely either individual episodes and/or sub-episodes of slow earthquake phenomena that go undetected.

3.2. Scaling Properties

Along-strike lengths (L) and along-dip widths (W) of the SEC rupture areas indicate that their aspect ratios (L/W) center around 1 (Figure 3a), similar to a recent slow-slip aspect-ratio study and regular earthquakes from around the world (Gao et al., 2012). From our dimension analysis, the 936 SECs in southwest Japan are limited in width (W_{max} = 45–50 km), as previously noted (Ide, 2010a). However, they are also limited along the fault strike (L < 100 km). The $L = W$ aspect ratio remains similar when isolating SECs by region along the Nankai subduction zone, with the exception of SECs that rupture across more than 1 region (<35 SECs). This suggests that the SECs we detected tend to remain in the same region from which they originate and highlights that there is some segmentation along the strike of the Nankai subduction zone. Bungo Channel and Northern Kii produce the largest SECs in terms of rupture area on average, consistent with their geodetically observed slow slip events (Sekine et al., 2010), while Southern Kii and Eastern Shikoku produce the smallest (Aiken & Obara, 2021). However, a region with fewer SECs does not appear to produce spatially larger SECs, i.e., does not accumulate stress as larger slow earthquake asperities. The SEC rupture areas (A) when compared to their seismic moments (M_0) follows a scaling law of $M_0 \sim A^{1.6}$ (Figure 3b), similar to regular earthquakes, i.e., $M_0 \sim A^{3/2}$ (Kanamori & Brodsky, 2004; Michel et al., 2019). SEC seismic moment also appears to scale with their durations as $M_0 \sim \tau^2$ (Figure 3c), a scaling which lies between the typically expected scaling of $M_0 \sim \tau$ for slow earthquake phenomena and $M_0 \sim \tau^3$ for fast, regular earthquakes

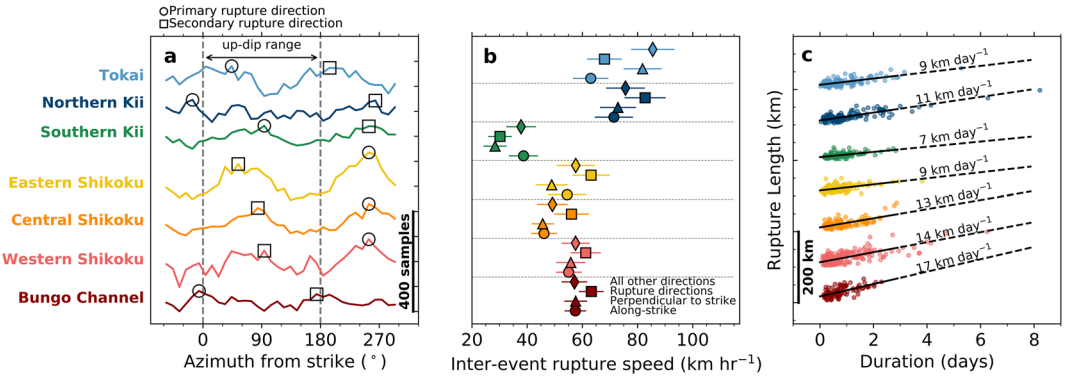

Figure 4. Rupture directivity and speeds. (a) Distribution of successive event azimuths by region along the Nankai subduction zone (West to East = bottom to top). Dashed gray lines mark the average trench strike determined from principal component analysis of events shown in Figure 1. Primary and secondary rupture directions are the two highest peaks of the azimuthal distributions (circle and square, respectively). Up-dip range is marked by the horizontal arrow. A scale of 200 samples is indicated for measuring peak-to-peak differences, as the distributions have been offset relative to one another. (b) Mean successive event ruptures speed for along-strike (circles), up-dip/down-dip (triangles), primary and secondary rupture directions (squares), and all other directions (diamonds). The rupture speeds are apparent speeds and log-normally distributed (Figure S9); Values shown are taken from the log distribution. (c) Average along-strike migration speed by region estimated as the fit of SEC rupture length versus SEC duration. A scale of 200 km is provided for rupture lengths, as they have been offset by 100 km for each region. In plot (a)–(c), colors match the region name shown in (a).

(Ide et al., 2007). This moment-duration scaling is, however, weakly correlated perhaps because the seismic moments are a cumulative estimate from the tremor and LFEs in a SEC and because tremor and LFEs have different reported event magnitude types (see Supporting Information). Thus, the SEC magnitudes are likely underestimated, due to poor efficiency in seismic radiation. Indeed, 3 to 4 orders of magnitude difference has been observed when scaling LFE seismic moment rate with geodetic moment rate (Frank & Brodsky, 2019). Despite the difference in estimated moment, the similarity in scaling shown in Figure 3 suggests that the SECs are fractal in nature, and their static stress drop is expected to be roughly constant along the Nankai subduction zone even when including small magnitude SECs, as has been observed for a compilation of slow events around the world, i.e., ~1 bar on average (Brodsky & Mori, 2007).

3.3. Rupture Directivity and Speed

Rupture migration patterns and speeds may delineate strong and weak patches along a fault zone. We calculated azimuths between successive pairs of events (i.e., tremor-tremor, tremor-LFE, LFE-tremor, or LFE-LFE) in each SEC and stacked these azimuths by region. The stacked azimuths yield both similarities and differences in the migration direction between events (Figure 4a). Neighboring regions in the center of Nankai subduction zone share similar distinguishable azimuthal peaks in how events within SECs tend to migrate, i.e., with preferred migration in the up-dip and down-dip directions. This is in contrast to slow earthquake phenomena migrating along-strike at longer time scales (e.g., Obara, 2010; Ghosh et al., 2012; Houston et al., 2011; Wech & Creager, 2011). Regions located on the edges of the study area have less distinctive event migration patterns and share no commonalities of preferred migration direction with neighboring regions. We note that the peak-to-peak difference between successive event migration in the along-strike and along-dip directions in Eastern Shikoku is ~2% of all the successive event azimuths samples of that region (~200 samples). Thus, while event migration in SECs seems to have a preference, this preference is quite weak.

Rupture migration patterns have been shown to be duration dependent such that at shorter time scales, there is a preferred rupture direction (Ide, 2012; Obara et al., 2012). However, in our study, we found no dependence between event migration within SECs and time elapsed between those events (Figure S8a). Thus, tremor and LFEs comprising SECs appear to migrate in a random way, and the inability to resolve this could be related to unknown tremor location errors.

Recent studies have also suggested that slow earthquakes rupture more quickly in the down-dip or up-dip direction compared to migrating along the strike of the fault (Ghosh et al., 2010; Shelly et al., 2007). Based on successive event rupture speeds, tremor and LFEs within the 936 SECs tend to migrate fastest in their preferred rupture direction (Figure 4b), a direction that varies between regions along the Nankai subduction zone (Figure 4a). Sometimes, the preferred rupture direction is the same as the along-strike or perpendicular-to-strike direction, e.g., Western Shikoku, and therefore, the successive event rupture speeds should be similar for the two cases. In our assessment, there is only a slight difference (<5–10 km h^{-1}), which we attribute to how we sample the rupture speeds by azimuth. Overall, the successive event rupture speeds range from 30-85 km hr^{-1} (Figure 4b) and tend to mirror those of previous studies in Japan (Obara et al., 2012; Shelly, 2010; Shelly et al., 2007) but are slightly slower than migration rates observed in Cascadia, i.e., up to 50–100 km h^{-1} (Ghosh et al., 2010). However, Cascadia migration rates are based on more macroscopic methods.

The 936 SECs have average along-strike rupture speeds ranging from 9 to 17 km day^{-1} depending on the region (Figure 4c), which is comparable to larger tremor episodes in Japan (Obara, 2010) and slow earthquake phenomena migration rates along the Cascadia subduction zone, i.e., 4–20 km day^{-1} (Ghosh et al., 2012; Houston et al., 2011; Wech & Creager, 2011). Short successive event timescales have been linked to faster rupture speeds (Houston et al., 2011; Ide, 2012; Obara et al., 2012), and in our study, successive events occurring within 1 h from each other exhibited rupture speeds on average around 150–200 km h^{-1} (Figure S8b), which is closer to rupture speeds observed in Cascadia for streaking tremor (Ghosh et al., 2010). While we did not observe streaking behavior directly, it could be inferred that tremor and LFEs in southwest Japan may exhibit streaking behavior as in Cascadia but without preferred direction. We could infer this for two reasons: (1) we observed no dependence between preferred successive event migration direction and time between events, and (2) shorter times between events exhibit faster rupture speeds. Thus, streaking behavior within SECs likely occurs randomly, which would suggest that the Nankai subduction zone is perhaps equally weak in all directions.

4. Discussion & Conclusions

We uncovered more than 900 slow earthquake clusters (SECs) between 2004 and 2013 along the Nankai subduction zone by applying a data-driven clustering method to a combined tremor and LFE catalog. The SEC occurrence rates varied by region along the Nankai subduction zone (Figure 2), but they exhibited similar scaling in their source properties (Figure 3). The small magnitude SECs we exposed here have small length scales compared to the typical tremor episode segmentation observed in Japan and Mexico (Maury et al., 2018; Obara, 2010) and episodic tremor and slip events along the Cascadia subduction zone (Michel et al., 2019). The SEC seismic moments scale with their durations as $M_0 \sim \tau^2$, which is between the typically expected scaling of $M_0 \sim \tau$ for slow earthquake phenomena and $M_0 \sim \tau^3$ for fast, regular earthquakes (Ide et al., 2007). Such an intermediate scaling has been suggested for a range of slipping phenomena (Peng & Gomberg, 2010), but our moment-duration scaling should be taken with caution as the seismic moment is estimated from seismic data only. Along the Nankai subduction zone, estimated SEC successive event rupture speeds varied between 30 and 85 km h^{-1}, depending on the rupture direction (Figure 4), which is similar to that observed for LFEs in Mexico (Frank et al., 2014) and within the range of streaking episodes observed along the Cascadia subduction zone (Ghosh et al., 2010; Wech and Creager, 2011), where larger magnitude slow earthquake phenomena tend to occur. In general, rapid streaks of tremor and LFEs are considered to be secondary events in larger slow earthquake phenomena and are common to Cascadia and Nankai (Houston et al., 2011), which supports the idea that our SEC catalog (Aiken and Obara, 2021) may contain sub-episodes of larger slow earthquake phenomena. However, the fact that we observed similar rupture speeds for small magnitude SECs all along the Nankai subduction zone highlights that rupture speed does not necessarily control SEC spatial extent or eventual magnitude. We note that our SECs predominantly contain tremor which provide less spatial and temporal resolution than an automatically detected LFE catalog, which might influence rupture speed and azimuthal calculations. However, even with the combined catalog containing mostly tremor, we were still able to identify similar rupture velocities and migration patterns observed in previous studies.

Finally, our SEC catalog (Aiken & Obara, 2021) likely represents either single episodes or sub-episodes of slow earthquake phenomena, such as ETS. For example, we detected four individual SECs that overlap spatially and temporally with a slow slip event occurring 16–20 April 2006 along the Nankai subduction zone. Such a case of small episodes has been observed in Cascadia where tremorless slow slip continued between tremor patches (Wech & Bartlow, 2014) and is suggestive of the intermittency of slow slip events that is obscured by the daily sampling rate of GPS positions (Frank et al., 2018). Nevertheless, we have generated a catalog of small magnitude SECs occurring along the Nankai subduction zone that has not yet been investigated. These small magnitude SECs confirm the fractal nature of slow earthquakes—in their energy, duration, and rupture areas. They also share similar source scaling to known larger slow earthquake phenomena (such as ETS) and regular earthquakes around the world. Therefore, a similar approach may be applied to other tremor catalogs to reveal small magnitude slow earthquakes occurring in the short-term that could improve our understanding of devastating earthquake cycles which occur in the long-term.

Conflict of Interest

The authors declare no competing interest(s).

Data Availability Statement

The tremor catalog dataset is freely available at http://www-solid.eps.s.u-tokyo.ac.jp/~idehara/wtd0/Welcome.html, last accessed 17 February 2020. The LFE catalog dataset is available from the NIED with user registration at http://www.hinet.bosai.go.jp/topics/JUICE/?LANG=en, last accessed 17 February 2020. The Southwest Japan slow earthquake cluster catalog developed in this study is openly available at https://osf.io/ywmg2. All figures and analyses were carried out using Python 3.6, which is open source.

Acknowledgments
C.Aiken conceived the idea and conducted the analyses. Both C.Aiken and K.Obara interpreted the data, contributed materials to the project, and participated in the manuscript writing process.

References

Aguiar, A. C., Melbourne, T. I., & Scrivner, C. W. (2009). Moment release rate of Cascadia tremor constrained by GPS. *Journal of Geophysical Research: Solid Earth*, *114*(7), B00A05. https://doi.org/10.1029/2008JB005909

Aiken, C., & Obara, K. (2021). Slow earthquakes detected via data-driven clustering of tremor and low-frequency earthquake catalogs. Open Science Framework Repository. Retreived from https://osf.io/ywmg2 (last accessed 1 April 2021).

Aiken, C., Obara, K., Peng, Z., Chao, K., & Maeda, T. (2014). Sweet spot tremor triggered by intraslab earthquakes in the Nankai subduction zone. *In American Geophysical Union Fall Meeting* (pp. S53C–S4525).

Aiken, C., & Peng, Z. (2014). Dynamic triggering of microearthquakes in three geothermal/volcanic regions of California. *Journal of Geophysical Research*, *119*(9), 6992–7009. https://doi.org/10.1002/2014JB011218

Bartlow, N. M., Miyazaki, S., Bradley, A. M., & Segall, P. (2011). Space-time correlation of slip and tremor during the 2009 Cascadia slow slip event. *Geophysical Research Letters*, *38*(18), L18309. https://doi.org/10.1029/2011GL048714

Brodsky, E. E., & Mori, J. (2007). Creep events slip less than ordinary earthquakes. *Geophysical Research Letters*, *34*(16), L16309. https://doi.org/10.1029/2007GL030917

Chestler, S. R., & Creager, K. C. (2017). A model for low-frequency earthquake slip. *Geochemistry, Geophysics, Geosystems*, *18*(12), 4690–4708. https://doi.org/10.1002/2017GC007253

Dragert, H., Wang, K., & James, T. S. (2001). A silent slip event on the deeper Cascadia subduction interface. *Science*, *292*(5521), 1525–1528. https://doi.org/10.1126/science.1060152

Frank, W. B., & Brodsky, E. E. (2019). Daily measurement of slow slip from low-frequency earthquakes is consistent with ordinary earthquake scaling. *Science Advances*, *5*(10), eaaw9386. https://doi.org/10.1126/sciadv.aaw9386

Frank, W. B., Radiguet, M., Rousset, B., Shapiro, N. M., Husker, A. L., Kostoglodov, V., et al. (2015). Uncovering the geodetic signature of silent slip through repeating earthquakes. *Geophysical Research Letters*, *42*(8), 2774–2779. https://doi.org/10.1002/2015GL063685

Frank, W. B., Rousset, B., Lasserre, C., & Campillo, M. (2018). Revealing the cluster of slow transients behind a large slow slip event. *Science Advances*, *4*(5), eaat0661. https://doi.org/10.1126/sciadv.aat0661

Frank, W. B., Shapiro, N. M., Husker, A. L., Kostoglodov, V., Romanenko, A., & Campillo, M. (2014). Using systematically characterized low-frequency earthquakes as a fault probe in Guerrero, Mexico. *Journal of Geophysical Research: Solid Earth*, *119*(10), 7686–7700. https://doi.org/10.1002/2014JB011457

Gao, H., Schmidt, D., & Weldon, R. J., Jr (2012). Scaling relationships of source parameters for slow slip events. *Bulletin of the Seismological Society of America*, *102*(1), 352–360. https://doi.org/10.1785/0120110096

Ghosh, A., Vidale, J. E., & Creager, K. C. (2012). Tremor asperities in the transition zone control evolution of slow earthquakes. *Journal of Geophysical Research*, *117*, B10301. https://doi.org/10.1029/2012JB009249

Ghosh, A., Vidale, J. E., Sweet, J. R., Creager, K. C., Wech, A. G., Houston, H., & Brodsky, E. E. (2010). Rapid, continuous streaking of tremor in Cascadia. *Geochemisty, Geophysics, Geosystems*, *11*(12), Q12010. https://doi.org/10.1029/2010GC003305

Hirose, H., Asano, Y., Obara, K., Kimura, T., Matsuzawa, T., Tanaka, S., & Maeda, T. (2010). Slow earthquakes linked along dip in the Nankai subduction zone. *Science*, *330*(6010), 1502. https://doi.org/10.1126/science.1197102

Hirose, H., & Obara, K. (2010). Recurrence behavior of short-term slow slip and correlated nonvolcanic tremor episodes in western Shikoku, southwest Japan. *Journal of Geophysical Research: Solid Earth*, *115*(B6), B00A21. https://doi.org/10.1029/2008JB006050

Houston, H., Delbridge, B. G., Wech, A. G., & Creager, K. C. (2011). Rapid tremor reversals in Cascadia generated by a weakened plate interface. *Nature Geoscience*, *4*, 404–409. https://doi.org/10.1038/ngeo1157

Husker, A., Frank, W. B., Gonzalez, G., Avila, L., Kostoglodov, V., & Kazachkina, E. (2019). Characteristics tectonic tremor activity observed over multiple slow slip cycles in the Mexican subduction zone. *Journal of Geophysical Research*, *124*(1), 599–608. https://doi.org/10.1029/2018JB016517

Ide, S. (2010a). Quantifying the time function of nonvolcanic tremor based on a stochastic model. *Journal of Geophysical Research: Solid Earth*, *115*(B8), B08313. https://doi.org/10.1029/2009JB000829

Ide, S. (2010b). Striations, duration, migration, and tidal response in deep tremor. *Nature*, *466*, 356–359. https://doi.org/10.1038/nature09251

Ide, S. (2012). Variety and spatial heterogeneity of tectonic tremor worldwide. *Journal of Geophysical Research*, *117*(B3), B03302. https://doi.org/10.1029/2011JB008840

Ide, S., Beroza, G., Shelly, D. R., & Uchide, T. (2007). A scaling law for slow earthquakes. *Nature*, *447*, 76–79. https://doi.org/10.1038/nature05780

Idehara, K., Yabe, S., & Ide, S. (2014). Regional and global variations in the temporal clustering of tectonic tremor activity. *Earth Planets and Space*, *66*, 66. https://doi.org/10.1186/1880-5981-66-66

Kanamori, H., & Brodsky, E. E. (2004). The physics of earthquakes. *Reports on Progress in Physics*, *67*(8), 1429–1496. https://doi.org/10.1088/0034-4885/67/8/R03

Kano, M., Aso, N., Matsuzawa, T., Ide, S., Annoura, S., Arai, R., et al. (2018). Development of a slow earthquake database. *Seismological Research Letters*, *89*(4), 1566–1575. https://doi.org/10.1785/0220180021

Lay, T., & Wallace, T. C. (1995). Modern global seismology (1st ed.,Vol. 58). London: Academic Press.

Maury, J., Ide, S., Cruz-Atienza, V. M., & Kostoglodov, V. (2018). Spatiotemporal variations in slow earthquakes along the Mexican subduction zone. *Journal of Geophysical Research: Solid Earth*, *123*(2), 1559–1575. https://doi.org/10.1002/2017JB014690

Michel, S., Gualandi, A., & Avouac, J.-P. (2019). Similar scaling laws for earthquakes and Cascadia slow-slip events. *Nature*, *574*, 522–526. https://doi.org/10.1038/s41586-019-1673-6

Obara, K. (2002). Nonvolcanic deep tremor associated with subduction in southwest Japan. *Science*, *296*(5573), 1679–1681. https://doi.org/10.1126/science.1070378

Obara, K. (2010). Phenomenology of deep slow earthquake family in southwest Japan: Spatiotemporal characteristics and segmentation. *Journal of Geophysical Research*, *115*(B8), B00A25. https://doi.org/10.1029/2008JB006048

Obara, K., Hirose, H., Yamamizu, F., & Kasahara, K. (2004). Episodic slow slip events accompanied by non-volcanic tremors in southwest Japan subduction zone. *Geophysical Research Letters*, *31*(23), L23602. https://doi.org/10.1029/2004GL020848

Obara, K., Matsuzawa, T., Tanaka, S., & Maeda, T. (2012). Depth-dependent mode of tremor migration beneath Kii Peninsula, Nankai subduction zone. *Geophysical Research Letters*, *39*(10), L10308. https://doi.org/10.1029/2012GL051420

Ozawa, S., Murakami, M., Kaidzu, M., Tada, T., Sagiya, T., Hatanaka, Y., et al. (2002). Detection and monitoring of ongoing aseismic slip in the Tokai region, central Japan. *Science*, *298*(5595), 1009–1012. https://doi.org/10.1126/science.1076780

Peng, Z., & Gomberg, J. (2010). An integrated perspective of the continuum between earthquakes and slow-slip phenomena. *Nature Geoscience*, *3*, 599–607. https://doi.org/10.1038/ngeo940

Rogers, G., & Dragert, H. (2003). Episodic tremor and slip on the Cascadia subduction zone: The chatter of silent slip. *Science*, *300*(5627), 1942–1943. https://doi.org/10.1126/science.1084783

Sekine, S., Hirose, H., & Obara, K. (2010). Along-strike variations in short-term slow slip events in the southwest Japan subduction zone. *Journal of Geophysical Research*, *115*(B9), B00A27. https://doi.org/10.1029/2008JB006059

Shelly, D. R. (2010). Migrating tremors illuminate complex deformation beneath the seismogenic San Andreas fault. *Nature*, *463*, 648–652. https://doi.org/10.1038/nature08755

Shelly, D. R., Beroza, G. C., & Ide, S. (2007). Complex evolution of transient slip derived from precise tremor locations in western Shikoku. *Geochemistry, Geophysics, Geosystems*, *8*(10), Q10014. https://doi.org/10.1029/2007GC001640

Shelly, D. R., Hill, D. P., Peng, Z., & Aiken, C. (2011). Triggered creep as a possible mechanism for delayed dynamic triggering of tremor and earthquakes. *Nature Geoscience*, *4*, 384–388. https://doi.org/10.1038/ngeo1141

Wech, A. G., & Bartlow, N. M. (2014). Slip rate and tremor genesis in Cascadia. *Geophysical Research Letters*, *41*(2), 392–398. https://doi.org/10.1002/2013GL058607

Wech, A. G., & Creager, K. C. (2011). A continuum of stress, strength and slip in the Cascadia subduction zone. *Nature Geoscience*, *4*, 624–628. https://doi.org/10.1038/ngeo1215

Zaliapin, I., & Ben-Zion, Y. (2013). Earthquake clusters in southern California I: Identification and stability. *Journal of Geophysical Research: Solid Earth*, *118*(6), 2865–2877. https://doi.org/10.1002/jgrb.50179